Inorganic Chemistry

Communication

pubs.acs.org/IC

# The Presence of Fast-Exchanging Proton Species in Aqueous Solutions of paraCEST Agents Can Impact Rate Constants Measured for Slower Exchanging Species When Fitting CEST Spectra to the Bloch Equations

Osasere M. Evbuomwan,*[,†] Joohwan Lee,[†] Mark Woods,[‡,§] and A. Dean Sherry*[,†,#]

[†]Department of Chemistry, University of Texas at Dallas, 800 West Campbell Road, Richardson, Texas 75080, United States

[‡]Department of Chemistry, Portland State University, 1719 SW 10th Avenue, Portland, Oregon 97201, United States

[§]Advanced Imaging Research Center, Oregon Health and Science University, 3181 SW Sam Jackson Park Road, Portland, Oregon 97239, United States

[#]Advanced Imaging Research Center, UT Southwestern Medical Center, 5323 Harry Hines Boulevard, Dallas, Texas 75235, United States

Supporting Information

**ABSTRACT:** LnDOTA-tetraamide complexes typically exist in solution as a mixture of square-antiprismatic (SAP) and twisted square-antiprismatic (TSAP) coordination isomers. In most cases, the SAP isomer, which is preferred for CEST imaging, predominates, and the presence of the minor TSAP isomer is assumed to have little influence on quantitative measures of the water-exchange rate constant for the SAP isomer. Here, we sought to confirm the validity of this assumption by mixing two chelates with different SAP and TSAP isomer populations while measuring the water-exchange rate constant of the SAP isomer. The results show that an increase in the population of the TSAP isomer in solution results in as much as a 30% overestimation of the water-exchange rate constant for the SAP isomer when CEST spectra are fit to the Bloch equations. This effect was shown to be significant only when the TSAP isomer population exceeded 50%.

LnDOTA-tetraamide complexes have been widely studied as paramagnetic chemical exchange transfer (paraCEST) contrast agents owing to their slow-to-intermediate water-exchange kinetics.[1−3] Slow water exchange between a $Ln^{3+}$-bound water molecule and bulk water combined with a large lanthanide-induced paramagnetic shift (LIS) in the bound water resonance are highly beneficial for CEST imaging applications. In some cases, dissociation of the $Ln^{3+}$-bound water molecule is so slow that the bound water resonance can be observed by high-resolution $^1$H NMR.[4,5] This slow water-exchange resonance can be selectively saturated using various frequency-selective RF schemes to reduce the intensity of the bulk water pool of protons following chemical exchange.

LnDOTA-tetraamide complexes can adopt either the monocapped square-antiprismatic (SAP) or monocapped twisted square-antiprismatic (TSAP) geometry, which interconvert by a macrocylic ring flip or rotation of the pendant arms.[6,7] The more compact nature of the SAP isomer results in a larger LIS in the proton resonances and slower water exchange, often up to 2 orders of magnitude slower than that in the TSAP isomer.[8,9] Hence, LnDOTA-tetraamide chelates that predominantly adopt the SAP geometry are highly preferred for paraCEST applications. While only a few methods for controlling the coordination geometry of LnDOTA-like chelates have been reported,[10−12] the majority of the LnDOTA-tetraamide complexes studied as paraCEST agents exist in solution as a mixture of SAP and TSAP isomers. The CEST signal from the SAP isomer is assumed to be independent of the presence and kinetics of water exchange in the TSAP isomer. Bloch simulations reported by Woessner et al.[13] predict that the mere presence of a fast-exchanging proton or water molecule in a system will impact the CEST efficiency of a slower-exchanging component. In this work, we sought to evaluate the magnitude of this effect experimentally by measuring the CEST properties of samples containing variable amounts of SAP [Eu-(**1**)] versus TSAP [Eu-(**2**)] species (Chart 1).

High-resolution $^1$H NMR spectroscopy was used to quantify the relative amounts of the SAP and TSAP isomers by taking advantage of the known chemical shifts of their respective macrocyclic axial ring protons ($H_4$ protons). For $Eu^{3+}$DOTA-tetraamide chelates, an $H_4$ proton resonance near 25 ppm is characteristic of the SAP isomer, while a resonance near 10 ppm

**Chart 1. Structures of the $Eu^{3+}$ Complexes Used in This Study**

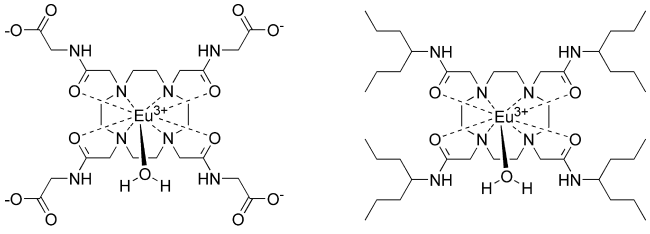


**Received:** June 3, 2014
**Published:** September 11, 2014

   dx.doi.org/10.1021/ic501290q | *Inorg. Chem.* 2014, 53, 10012−10014

signifies the presence of the TSAP isomer. Integration of the area under these peaks followed by normalization provided the relative proportion of each coordination isomer for each of the pure Eu-(**1**) and Eu-(**2**) complexes (Figure 1).

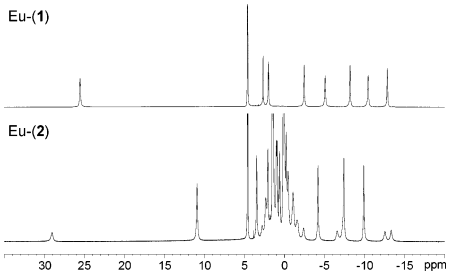


**Figure 1.** High-resolution $^1$H NMR spectra of Eu-(**1**) (top) and Eu-(**2**) (bottom) showing the relative amounts of SAP and TSAP isomers. Spectra were recorded in $D_2O$ at 298 K and 400 MHz.

It is evident that the populations of the SAP and TSAP isomers in the two samples are dramatically different, with Eu-(**1**) existing mostly as the SAP isomer (>99%) and Eu-(**2**) predominantly adopting the TSAP geometry (~78%). This preference for the TSAP isomer was ascribed to the increased steric demand at the lanthanide ion brought about by the bulkiness of the amide heptyl groups.[14] The slow water-exchange kinetics and larger $Eu^{3+}$-bound water chemical shift of the SAP isomer indicate that Eu-(**1**) would exhibit more favorable CEST properties because it preferentially adopts this coordination geometry.

CEST spectra of five aqueous samples containing varying proportions of Eu-(**1**) and Eu-(**2**) were recorded at pH 7 and 298 K (Figure 2a). The total $Eu^{3+}$ concentration and the sample volume were maintained at 20 mM and 500 $\mu$L, respectively, to maintain constant bulk water proton $T_1$ and $T_2$ values. For comparison purposes, CEST spectra of four samples containing different concentrations of only Eu-(**1**) were also recorded (Figure 2b). In a qualitative sense, the addition of the more rapidly exchanging Eu-(**2**) species to the more slowly exchanging Eu-(**1**) species has an impact on both the line width and intensity of the Eu-(**1**) exchange peak at 55 ppm (parts a vs b in Figure 2). Figure 2b shows the effect of simple dilution of Eu-(**1**) for comparison. It is noteworthy that the width of the bulk water peak (at 0 ppm) also broadens as more Eu-(**2**) is added, whereas simple dilution of Eu-(**1**) alone results in a sharpening of this peak. These observations show that the bound water CEST signal from the SAP isomer of Eu-(**1**) is indeed influenced by the presence of a second rapidly exchanging chemical species.

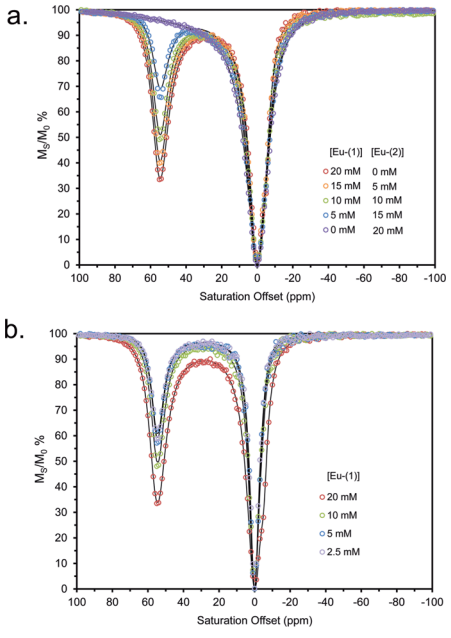


**Figure 2.** (a) CEST spectra of aqueous solutions containing different proportions of Eu-(**1**) and Eu-(**2**) with [$Eu^{3+}$] = 20 mM. (b) CEST spectra of Eu-(**1**) at different concentrations in the absence of Eu-(**2**). Spectra were recorded at 298 K, pH 7, $B_1$ = 18.8 $\mu$T, and saturation time = 6 s.

The CEST spectrum of Eu-(**2**) alone (Figure 2a) does not show distinct water-exchange peaks from either the minor SAP isomer (~22%) or the major TSAP isomer (~78%) but rather shows an asymmetric bulk water peak with a broad component on the low-field side. Such CEST spectra are characteristic of samples that contain only fast-exchanging water species.[15,16] This observation confirms that water exchange in both the SAP and TSAP isomers of Eu-(**2**) occurs much more rapidly in this complex than in Eu-(**1**).

Next, we tested whether the qualitative changes observed in the CEST spectra of Eu-(**1**) would result in the quantitative evaluation of water-exchange rate constants as determined by two common methods.[13,18] The CEST spectrum of 100% Eu-(**1**) was first fit to the Bloch equations[13] with three exchanging pools (the SAP-bound water, the amide protons, and bulk water). This fit gave a bound water lifetime of 154 $\mu$s, identical with the value previously reported for this compound at the same temperature.[18] It was found that including the exchanging amide protons as a separate pool in the model had little impact on the measured water-exchange rate constant, likely because the amide protons are not shifted far from the bulk water peak.

The water-exchange kinetics of Eu-(**1**) were then assessed using the Bloch equations in samples containing Eu-(**2**) as well. CEST spectra were fit to similar three-pool Bloch exchange models: bulk water, the SAP-bound water pool, and the invisible TSAP-bound water pool. In each case, the results of the fitting suggest that water exchange in Eu-(**1**) accelerates as more Eu-(**2**) is added (Figure 3); the calculated water-exchange rate constant for Eu-(**1**) was up to 30% higher at the highest concentration of added Eu-(**2**).

Previous studies of Eu-(**1**) showed that the CEST spectrum from the $Eu^{3+}$-bound water exchange is constant between pH 5–

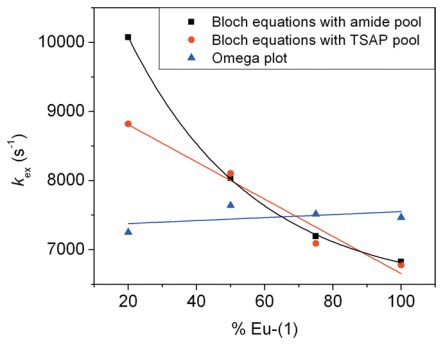


**Figure 3.** Comparison of water-exchange rate constants for the SAP isomer of Eu-(**1**) as obtained by fitting of the CEST spectra ($B_1$ = 18.8 $\mu$T) to the Bloch equations (two models) and by use of the omega plot method.


dx.doi.org/10.1021/ic501290q | *Inorg. Chem.* 2014, 53, 10012–10014

8 so catalysis by some undefined prototropic exchange mechanism is unlikely.[17] It seems probable that water exchange in the SAP isomer of Eu-(**1**) is actually constant with or without Eu-(**2**), but it is the fitting procedure that is the source of the variable calculated water-exchange rate constants. To test this, water-exchange rate constants for the SAP isomer of Eu-(**1**) were also measured using the concentration-independent omega plot method.[18] Here, an evaluation of the water-exchange rate constant is based solely on changes in the CEST intensity as the power of the applied $B_1$ pulse is varied. The resulting omega plots for the four samples containing variable amounts of Eu-(**1**) and Eu-(**2**) are shown in Figure S4 in the Supporting Information, and the calculated water-exchange rate constants are represented by the points on the blue line (Figure 3). It is evident from these data that water exchange in Eu-(**1**) is not only independent of the concentration as expected for a dissociative water-exchange mechanism but also independent of the presence of the faster water-exchange species, Eu-(**2**). These results reflect a limitation in the way the Bloch model calculates exchange rate constants from CEST spectra.[13] The exchange rate constants determined by Bloch fitting are heavily influenced by the width of each CEST exchange peak including that of bulk water. The effect of adding Eu-(**2**) to a sample of Eu-(**1**) was to shorten the $T_2$ of bulk water and therefore increase the width of the bulk water-exchange peak. This resulted in improper fitting by the Bloch fitting method to yield rate constants up to 50% too large. The concentration-independent omega plot method provides a more direct measure of water-exchange rate constants for the species in question in the presence of other rapidly exchanging species. These results have implications for in vivo applications of paraCEST agents because there will always be several fast-exchanging proton species in tissue. In this case, the omega plot method is the obvious method of choice to measure water-exchange kinetics.

## ■ ASSOCIATED CONTENT

### Ⓢ Supporting Information

Experimental details, CEST spectra, and omega plots. This material is available free of charge via the Internet at http://pubs.acs.org.

## ■ AUTHOR INFORMATION


### Corresponding Authors

*E-mail: osaseree@mit.edu.

*E-mail: dean.sherry@utsouthwestern.edu.


### Notes

The authors declare no competing financial interest.

## ■ ACKNOWLEDGMENTS

The authors acknowledge financial support from the National Institutes of Health (Grants CA-115531, RR-02584, and EB-00482) and the Robert A. Welch Foundation (Grant AT-584).

## ■ REFERENCES


(1) Sherry, A. D.; Woods, M. *Annu. Rev. Biomed. Eng.* **2008**, *10*, 12.1−12.21.

(2) Woods, M.; Donald, E. W. C.; Sherry, A. D. *Chem. Soc. Rev.* **2006**, *35*, 500−511.

(3) Zhang, S. R.; Merritt, M.; Woessner, D. E.; Lenkinski, R. E.; Sherry, A. D. *Acc.. Chem. Res.* **2003**, *36*, 783−790.

(4) Zhang, S.; Winter, P.; Wu, K.; Sherry, A. D. *J. Am. Chem. Soc.* **2001**, *123*, 1517−1518.

(5) Zhang, S.; Wu, K.; Biewer, M. C.; Sherry, A. D. *Inorg. Chem.* **2001**, *40*, 4284−90.

(6) Aime, S.; Botta, M.; Ermondi, G. *Inorg. Chem.* **1992**, *31*, 4291−4299.

(7) Hoeft, S.; Roth, K. *Chem. Ber.* **1993**, *126*, 869−873.

(8) Aime, S.; Barge, A.; Bruce, J. I.; Botta, M.; Howard, J. A. K.; Moloney, J. M.; Parker, D.; de Sousa, A. S.; Woods, M. *J. Am. Chem. Soc.* **1999**, *121*, 5762−5771.

(9) Woods, M.; Aime, S.; Botta, M.; Howard, J. A. K.; Moloney, J. M.; Navet, M.; Parker, D.; Port, M.; Rousseaux, O. *J. Am. Chem. Soc.* **2000**, *122*, 9781−9792.

(10) Woods, M.; Botta, M.; Avedano, S.; Wang, J.; Sherry, A. D. *Dalton Trans.* **2005**, 3829−3837.

(11) Woods, M.; Kovacs, Z.; Zhang, S. R.; Sherry, A. D. *Angew. Chem., Int. Ed.* **2003**, *42*, 5889−5892.

(12) Carney, C. E.; Tran, A. D.; Wang, J.; Schabel, M. C.; Sherry, A. D.; Woods, M. *Chem.—Eur. J.* **2011**, *17*, 10372−10378.

(13) Woessner, D. E.; Zhang, S. R.; Merritt, M. E.; Sherry, A. D. *Magn. Reson. Med.* **2005**, *53*, 790−799.

(14) Woods, M.; Mani, T.; Tircso, G.; Zhao, P. Y.; Sherry, A. D. *Inorg. Chem.* **2009**, *48*, 10338−10345.

(15) Mani, T.; Tircso, G.; Togao, O.; Zhao, P.; Soesbe, T. C.; Takahashi, M.; Sherry, A. D. *Contrast Media Mol. Imaging* **2009**, *4*, 183−191.

(16) Aime, S.; Barge, A.; Botta, M.; Parker, D.; DeSousa, A. S. *J. Am. Chem. Soc.* **1997**, *119*, 4767−4768.

(17) Aime, S.; Delli Castelli, D.; Terreno, E. *Angew. Chem., Int. Ed.* **2002**, *41*, 4334−4336.

(18) Dixon, W. T.; Ren, J. M.; Lubag, A. J. M.; Ratnakar, J.; Vinogradov, E.; Hancu, I.; Lenkinski, R. E.; Sherry, A. D. *Magn. Reson. Med.* **2010**, *63*, 625−632.